AIP | The Journal of Chemical Physics

Ionization of gases by a pulsed electron beam as studied by selffocusing. II. Polyatomic gases

Hidehiko Arai and Hiroshi Hotta

Citation: The Journal of Chemical Physics **75**, 2723 (1981); doi: 10.1063/1.442341
View online: http://dx.doi.org/10.1063/1.442341
View Table of Contents: http://scitation.aip.org/content/aip/journal/jcp/75/6?ver=pdfcov
Published by the AIP Publishing

Ionization of gases by a pulsed electron beam as studied by self-focusing. II. Polyatomic gases

Hidehiko Arai

Takasaki Radiation Chemistry Research Establishment, Japan Atomic Energy Research Institute, Takasaki, Gunma, 370-12 Japan

Hiroshi Hotta

Fukui Institute of Technology, Fukui, 910 Japan
(Received 5 March 1981; accepted 27 May 1981)

In order to analyze data on the self-focusing of a pulsed electron beam in polyatomic gases, the net current I_{net} in H_2, N_2, and CH_4 was computed self-consistently as functions of time in the pressure range between 5 and 300 Torr of these gases by using swarm parameters. The computational result indicates that the larger dose D_{obs}, observed by a piled dosimeter on the beam axis, is attributed to the larger I_{net}, which is mainly determined by a mean ionization time t_i for secondary ionization by the electric field induced by the pulsed beam. When values of D_{obs} for different gases are compared at the same pressure, the larger D_{obs} is given by the larger t_i. This relationship is demonstrated for several polyatomic gases by estimating t_i from various parameters in a function of secondary electron energy or E/p such as the electron drift velocity, the first Townsend ionization coefficient, the ionization cross section, and so on. For the short pulse duration of a Febetron 706, electron–ion recombination processes scarcely affect I_{net} except at high pressures of some polyatomic gases, while the effect of electron-attachment processes is appreciable in SF_6, CCl_2F_2, and N_2O.

INTRODUCTION

In a preceding paper (part I),[1] it has been shown that, for monatomic gases, the maximum dose (D_{obs}) of the depth–dose curve in a piled dosimeter given by a pulsed electron beam of a Febetron 706 (tube 5515)[2] can be interpreted in terms of the net current I_{net}, which is mainly determined by a mean ionization time t_i. The value of I_{net} has been calculated with the following equations:

$$I_{net}(t) = I_b(t) + I_{back}(t) , \tag{1}$$

$$I_{back}(t) = \pi r_0 E_z(t)\sigma_e(t) , \tag{2}$$

$$E_z(t) = -\frac{2}{c^2}\left(\frac{1}{2} + \ln\frac{R}{r_0}\right)\frac{dI_{net}(t)}{dt} , \tag{3}$$

$$\sigma_e(t) = \frac{e^2 n_e(t)}{n_0(2m)^{1/2} Q_m(\bar\epsilon)\bar\epsilon^{1/2}} , \tag{4}$$

$$\frac{dn_e(t)}{dt} = \frac{n_0\sigma_{ion}(E_b)I_b(t)}{\pi r_0^2 e} + \frac{n_e(t)}{t_i(t)} , \tag{5}$$

where I_b is the beam current assumed as in part I, I_{back} the plasma backward current, r_0 the beam radius assumed to be 0.6 cm, R the chamber radius (6.4 cm), E_z the longitudinal electric field induced along the beam coordinate z by the pulsed beam, c the velocity of light, σ_e the plasma conductivity of the irradiated medium gas, m the electron rest mass, e the electron charge, n_0 the number density of gas molecules, n_e the number density of secondary electrons, and Q_m the momentum transfer cross section for electrons with mean kinetic energy $\bar\epsilon$. The total ionization cross section $\sigma_{ion}(E_b)$ for the beam electron with energy E_b is estimated for $\bar{E}_b = 480$ keV from the Rieke–Prepejchal parameters.[3] The mean ionization time t_i for secondary ionization has been determined as a function of E/p for some gases by Felthenthal and Proud.[4] For other gases, t_i can be estimated by[4]

$$1/(pt_i) = w(\alpha/p - \eta/p) , \tag{6}$$

where α is the first Townsend ionization coefficient, η the electron-attachment coefficient, and w the electron drift velocity. It has been demonstrated from the calculated I_{net} that D_{obs} can be expressed approximately as

$$D_{obs} \propto \int \frac{I_b(t) I_{net}(t)}{\epsilon_b^2} dt , \tag{7}$$

where $\pi\epsilon_b$ is the beam emittance. Thus, the larger D_{obs} corresponds to the larger I_{net}, which is given by the smaller I_{back} for $dI_{net}/dt > 0$ from Eqs. (1)–(3). This means that the larger D_{obs} is given by a gas with the larger t_i for $dI_{net}/dt > 0$.

The similar computation was carried out for H_2, N_2, and CH_4. In the present paper, data on D_{obs} for various polyatomic gases[5–7] are discussed on the basis of the computational result for these gases.

COMPUTATION FOR H_2, N_2, and CH_4

In the computation, the parameters r_0, $I_b(t)$, and $\sigma_{ion}(E_b)$ were used on the same assumptions as made in part I.[1] Literature values were used for the following parameters; w,[8] α/p,[9] D_L/μ,[10] and Q_m[11] for H_2; w,[8] α/p,[12] D_L/μ,[13] and Q_m[11] for N_2; and w,[14–16] α/p,[17] D_L/μ,[18] and Q_m[19,20] for CH_4. The value of $\bar\epsilon$ was estimated from data on D_L/μ on the assumption of the Maxwellian. For polyatomic gases, Eq. (5) was revised as

$$\frac{dn_e}{dt} = \underbrace{\frac{n_0\sigma_{ion}(E_b)}{e}\cdot\frac{I_b(t)}{\pi r_0^2}}_{\text{(term 1)}} + \underbrace{\frac{n_e(t)}{t_i(t)}}_{\text{(term 2)}}$$

$$\underbrace{-\alpha_r n_e(t) n_i(t)}_{\text{(term 3)}} \underbrace{- \alpha_{rd} n_e(t) n_d(t)}_{\text{(term 4)}} , \tag{8}$$

$$\frac{dn_i}{dt} = \frac{n_0\sigma_{ion}(E_b)}{e}\cdot\frac{I_b(t)}{\pi r_0^2} + \frac{n_e}{t_i} - \alpha_r n_e n_i - k_d n_i n_0^2 , \tag{9}$$

$$\frac{dn_d}{dt} = k_d n_i n_0^2 - \alpha_{rd} n_e n_d , \tag{10}$$

0021-9606/81/182723-07$01.00

where α_r and α_{rd} are the recombination coefficients (cm^3/s) between electron–ion and electron–dimer ion, respectively, and k_d is the rate constant of dimer ion formation. The number densities of ions and dimer ions are represented by n_i and n_d, respectively. We have assumed that the variation of α_r and α_{rd} with $\bar{\epsilon}$ is expressed as

$$\alpha_r(H_2^+) = 4.7\times 10^{-8}\bar{\epsilon}^{-0.40} \quad \text{(Ref. 21)},$$

$$\alpha_r(N_2^+) = 5.5\times 10^{-8}\bar{\epsilon}^{-0.65}, \quad \text{for } \bar{\epsilon} > 1 \text{ eV (Ref. 22)},$$

$$\alpha_{rd}(N_4^+) = 3.7\times 10^{-7}\bar{\epsilon}^{-0.65}, \quad \text{for } \bar{\epsilon} > 1 \text{ eV (Ref. 22)},$$

$$\alpha_r(CH_3^+) = 5.5\times 10^{-8}\bar{\epsilon}^{-0.93}, \quad \text{for } \bar{\epsilon} > 0.8 \text{ eV (Ref. 23)},$$

$$\alpha_{rd}(C_2H_5^+) = 9.5\times 10^{-8}\bar{\epsilon}^{-0.75}, \quad \text{for } \bar{\epsilon} > 1 \text{ eV (Ref. 23)},$$

and for formation processes of N_4^+ and $C_2H_5^+$:

$$N_2^+ + 2N_2 \rightarrow N_4^+ + N_2$$

$$(k_d = 8\times 10^{-29} \text{ molecule}^{-2}\,\text{cm}^6\,\text{s}^{-1}) \text{ (Ref. 24)},$$

$$CH_3^+ + CH_4 \rightarrow C_2H_5^+ + H_2$$

$$(k_d = 1\times 10^{-9}\ \text{cm}^3/\text{s}) \text{ (Ref. 25)}.$$

For hydrogen, only the association reaction of H^+ leading to H_3^+ is known.[24] However, the yield of H^+ is small in comparison with that of H_2^+ (about several percent).[26,27] Thus, the recombination of electron–H_3^+ was neglected in the calculation for H_2. Only the formation of CH_3^+ and $C_2H_5^+$ was assumed in the calculation for methane.

Computational results of $I_{net}(t)$ for H_2, N_2, and CH_4 are shown in Figs. 1, 2, and 3, respectively. They show that the calculated value of I_{net} at lower pressure is nearly constant after a certain time, as has been assumed previously as the t_B model.[5] The value of D_{obs} increases at first with increasing pressure in the low pressure region, and after passing the maximum it decreases abruptly at a certain pressure (usually 1–5 Torr) but increases again with further increasing pressure.[6,7] The curve of $I_{net}(t)$ varies according to the t_B model up to the pressure giving the minimum D_{obs}. In this region, $I_{net}(t)$ decreases with increasing pressure.

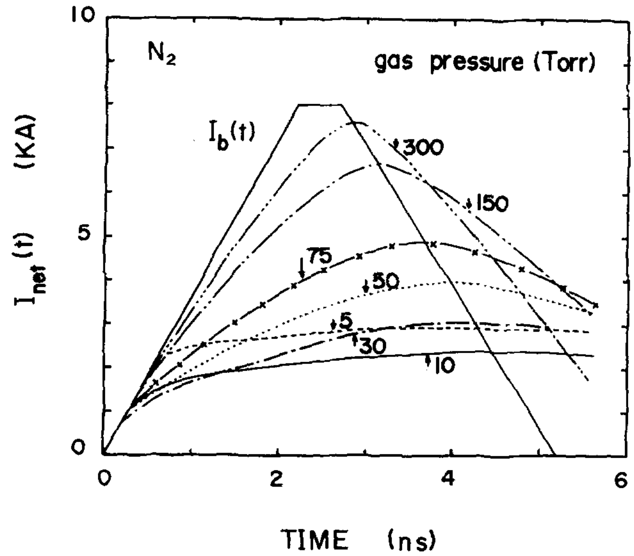

FIG. 2. The calculated net current $I_{net}(t)$ as a function of time for various pressures of N_2.

In the present paper, we are most interested in the higher pressure region in which D_{obs} increases gradually after passing the minimum. In this region, in Figs. 1–3, $I_{net}(t)$ increases appreciably with the lapse of time and also increases with increasing pressure. According to Eq. (7), D_{obs} should be proportional to the value of $\int I_b(t) I_{net}(t) dt$ if the variation of ϵ_b is ignored. In Fig. 4, values of this integral are plotted in an arbitrary unit by solid symbols for H_2, N_2, and CH_4 by using the calculated values of I_{net} in Figs. 1, 2, and 3, respectively, together with the curves of D_{obs} shown by open symbols. The curve of the integral represents fairly well the aspect of the curve of D_{obs}. However, when both the curves are compared at the pressure giving the minimum, the value

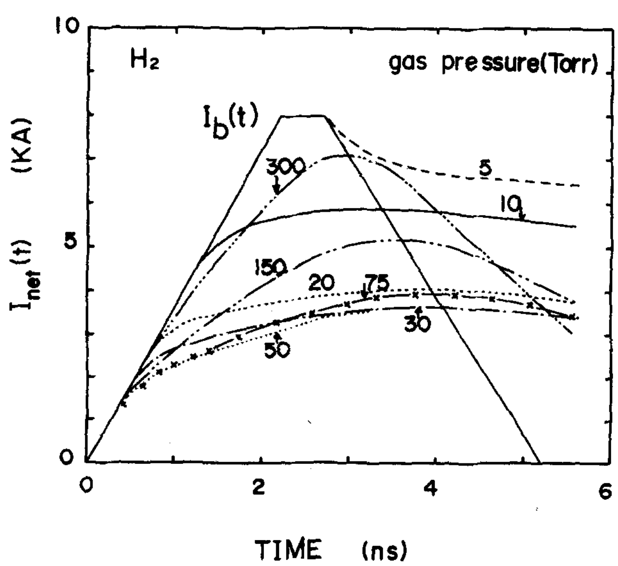

FIG. 1. The calculated net current $I_{net}(t)$ as a function of time for various pressures of H_2. The solid straight lines indicate the beam current $I_b(t)$.

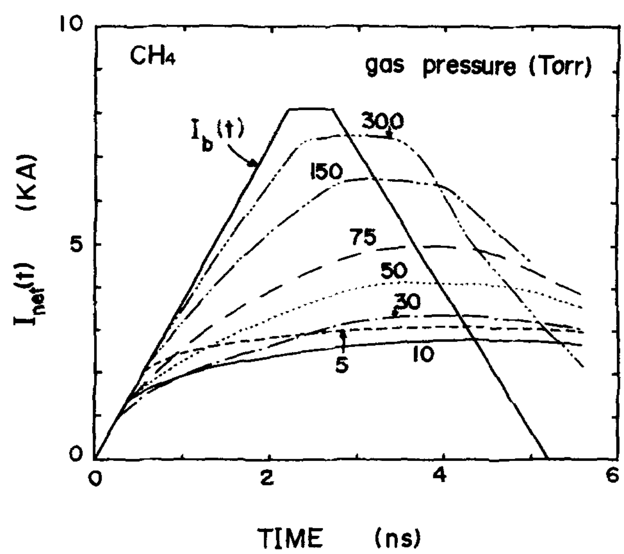

FIG. 3. The calculated net current $I_{net}(t)$ as a function of time for various pressures of CH_4.

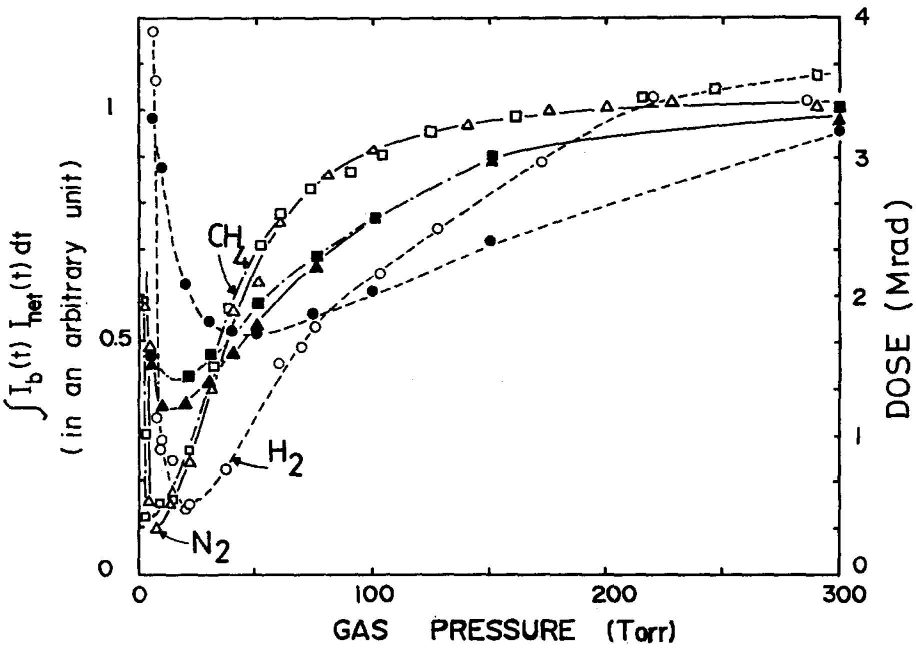

FIG. 4. D_{obs} at various pressures of H_2, N_2, and CH_4: o (H_2), Δ (N_2), and □ (CH_4). Solid marks [● (H_2), ▲ (N_2), and ■ (CH_4)] indicate the values of the integral in Eq. (7) in an arbitrary unit.

of the integral is relatively larger than that of D_{obs}. This can be fitted by using the correct value of ϵ_b as has been discussed in part I.[1] Consequently, the present computational result represents fairly well the phenomena induced by the pulsed beam in a gas chamber so that the calculated values of parameters such as I_{net}, n_e, and E/p, which are not easy to be measured, might be used semiquantitatively.

Curves of E_z/p calculated from the values of I_{net} in Figs. 1, 2, and 3 are shown as functions of t in Figs. 6, 7, and 8 for H_2, N_2, and CH_4, respectively. In the present computation, values of $\bar{\epsilon}$ are estimated from data on D_L/μ on the assumption of the Maxwellian as functions of the calculated E_z/p shown in Figs. 6–8. Such values of $\bar{\epsilon}$ at pressure of 30 Torr for three gases, as

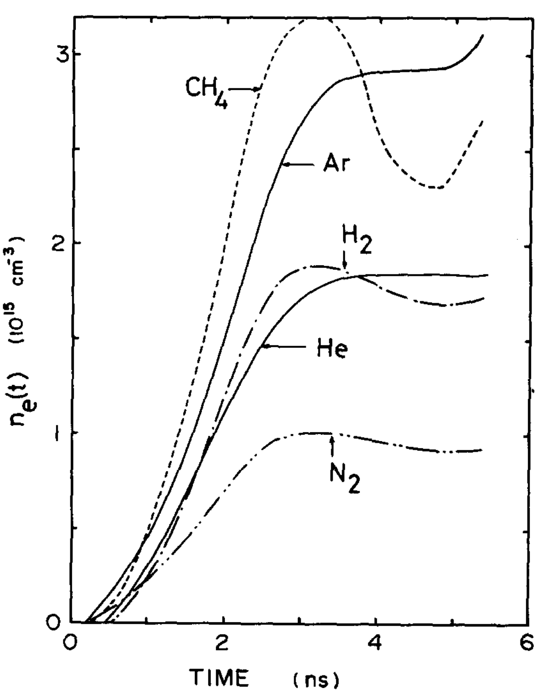

FIG. 5. The calculated number density $n_e(t)$ of produced secondary electrons as functions of time at 50 Torr of He (—), Ar (—), H_2 (- · -), N_2 (- · · · -), and CH_4 (----).

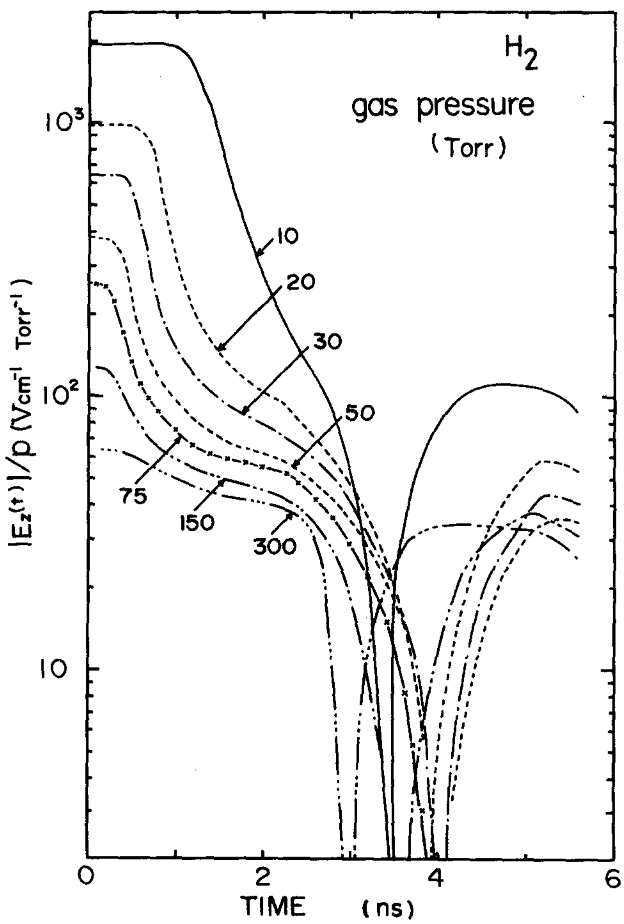

FIG. 6. The calculated $|E_z(t)|/p$ [$E_z(t)$: the induced longitudinal electric field] as functions of time for various pressures of H_2.

the representative, are shown as functions of t in Fig. 9, because we are interested mainly in the pressure region between 10 and 50 Torr in the present paper. Curves in Figs. 6–8 show that the value of E_z/p decreases abruptly for a short period. However, the actual value of $\bar{\epsilon}$ for this period might not so decrease as shown in Fig. 9 so that the value of t_i for this period may not vary abruptly according to such a calculated E_z/p because of the presence of the relaxation time of $\bar{\epsilon}$. The present computation, however, was carried out straightforwardly according to the calculated E_z/p without any correction.

The calculated value of $n_e(t)$ increased with increasing pressure and became the maximum at 75 Torr of H_2, 50 Torr of N_2, and 30 Torr of CH_4. The value decreased slightly with further increasing pressure. The value of n_e became the maximum at the pressure for which D_{obs} is nearly equal to 1 Mrad. Such a relationship of $n_e(t)$ between p or D_{obs} is common with He and Ar, whose curves are shown in detail in part I.[1] Then, the curve of $n_e(t)$ becomes almost the same irrespective of pressure for D_{obs} higher than 1 Mrad. Curves of $n_e(t)$ at 50 Torr are shown as functions of t in Fig. 5.

The contribution of each term to the total n_e in Eq. (8) is as follows, although the computation was carried out for a discrete value of p: The contribution of direct ionization (term 1) is less than 10% of electron avalanching (term 2) at 20–150 Torr of H_2, 5–50 Torr of N_2, and 5–100 Torr of CH_4. Furthermore, the contribution of recombination precesses (terms 3 and 4) at the peak of

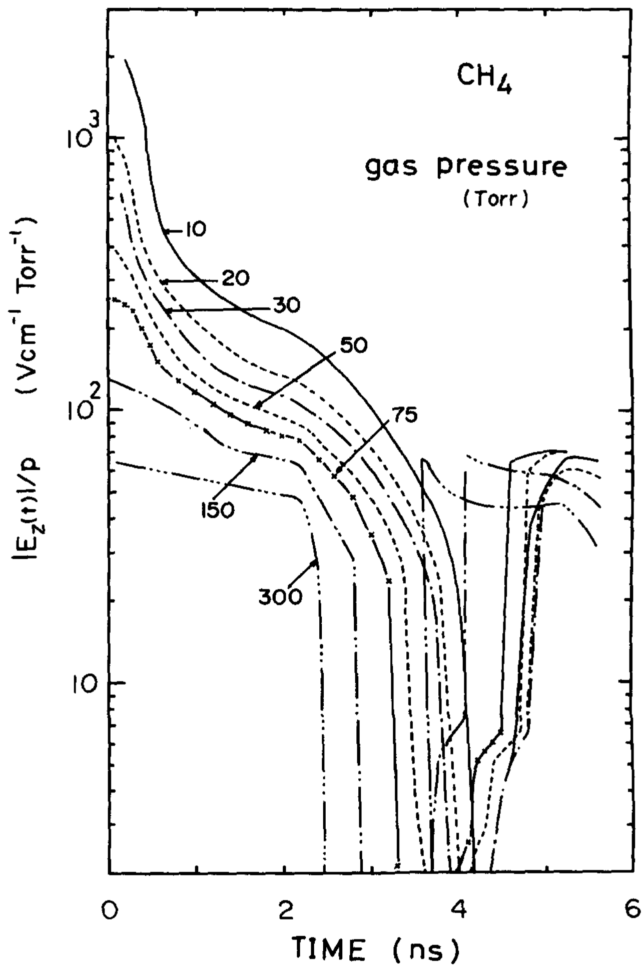

FIG. 8. The calculated $|E_z(t)|/p$ as functions of time for various pressures of CH_4.

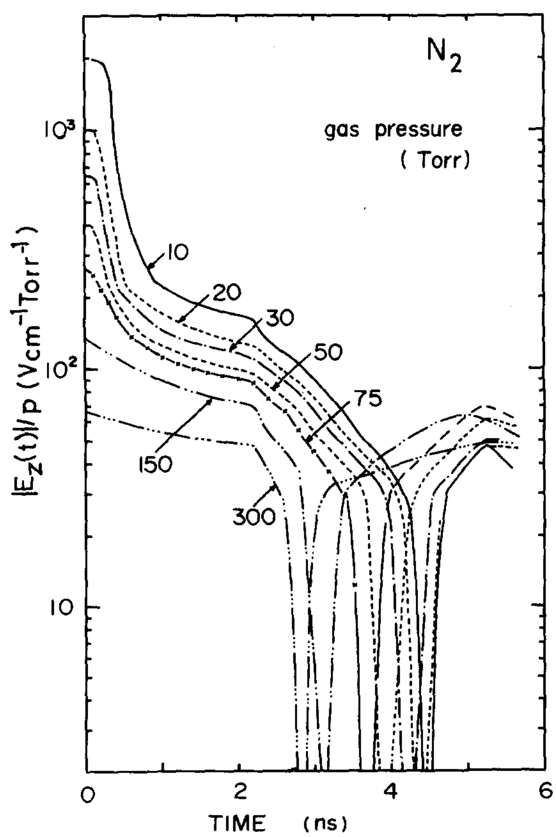

FIG. 7. The calculated $|E_z(t)|/p$ as functions of time for various pressures of N_2.

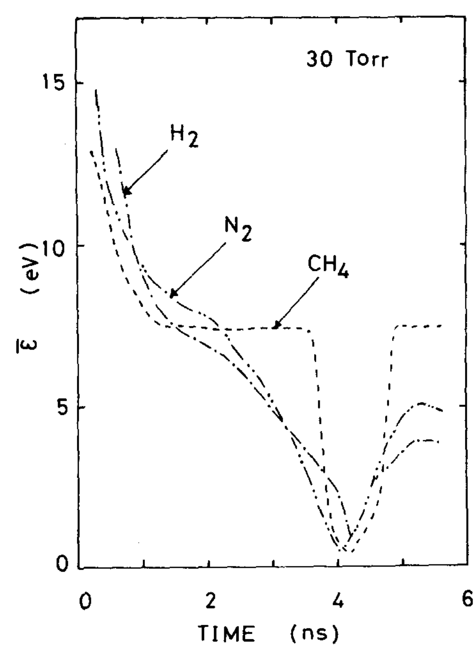

FIG. 9. The mean electron energy estimated at 30 Torr of H_2 (- · · -), N_2 (- · · · -), and CH_4 (----) as functions of time.

the pulsed beam (2.2 ns) is less than 10% of the total n_e at pressures below 300 Torr of the three gases. At higher pressure, however, the recombination contribution became large at 3 ns due to decreasing $\bar{\epsilon}$ in the low-E/p region and due to the large amount of dimer-ion formation. Some results are shown in Figs. 10 and 11. The number densities of secondary electrons (n_e), $N_2^+(n_i)$, and $N_4^+(n_d)$ at 30 and 300 Torr of N_2 are shown as functions of t in Fig. 10. At 300 Torr, most of N_2^+ becomes N_4^+ without recombination for the pulse duration. The similar curves of n_e, $n_i(CH_3^+)$, and $n_d(C_2H_5^+)$ at 30 and 300 Torr of CH_4 are shown in Fig. 11.

Generally speaking, since n_e is on the order of 10^{15} cm^{-3} as seen in Fig. 5, the half-life of secondary electrons for electron–ion recombination processes is less than 1 ns for α_r larger than 10^{-6} $cm^3\,s^{-1}$. Such large rate constants, are reported only for N_4^+,[28] O_4^+,[28] and CH_4^+ or CH_3^+[23] for thermal electrons and N_2O^+[29] for 0.04 eV electrons. Apparent recombination coefficients for N_2, CO_2, CH_4, and C_3H_8 for thermal electrons[30] are also larger than 10^{-6} $cm^3\,s^{-1}$ at 50 Torr. When α_r is reduced according to the $\bar{\epsilon}^{-0.5}$ law, the value may be on the order of 10^{-7} $cm^3\,s^{-1}$ even for these gases for the present experiments. Therefore, we can ignore the electron–ion recombination process at least for the ns pulse duration in the pressure region of interest.

DISCUSSION

It is concluded from Fig. 4 that the larger D_{obs} is given by the larger I_{net} which is due to the smaller I_{back} or $\sigma_e E_z$ from Eqs. (1), (2), and (7). From Eq. (4), $\sigma_e E_z$ is proportional to the product of $n_e/Q_m\bar{\epsilon}^{1/2}$ and E_z/p. The value of $Q_m(\bar{\epsilon})\bar{\epsilon}^{1/2}$ increases with increasing $\bar{\epsilon}$ and usually becomes nearly constant from a certain $\bar{\epsilon}$. Such plateau values are $(2-3)\times10^{-15}$ $cm^2\,eV^{0.5}$ for 1–10 eV of $\bar{\epsilon}$ (5–300 $V\,cm^{-1}\,Torr^{-1}$ of E/p) for H_2, $(2.5-4.5)\times10^{-15}$ $cm^2\,eV^{0.5}$ for 2–10 eV of $\bar{\epsilon}$ (1–150 $V\,cm^{-1}\,Torr^{-1}$ of E/p) for N_2, and 6.5×10^{-15} $cm^2\,eV^{0.5}$ for 7.4 eV (24–136 $V\,cm^{-1}\,Torr^{-1}$ of E/p) for CH_4. In Figs. 6–8, these E/p regions giving the plateau value are covered by the major part of the pulse duration. The difference of $Q_m(\bar{\epsilon})\bar{\epsilon}^{1/2}$ among gases must be noticed but the plateau values are not much different among gases except CH_4. Then, the aspect of D_{obs} can be analyzed mainly by E/p and n_e.

Since the larger I_{net} induces the larger E_z from Eq. (3), at the same pressure, the larger D_{obs} is associated with the larger E_z/p in spite of the smaller I_{back} because the larger D_{obs} corresponds to the smaller I_{back} as pointed out above. From Eqs. (2) and (4), this means that the larger D_{obs} is given by a gas with the smaller $n_e/Q_m\bar{\epsilon}^{1/2}$ at the same pressure. The smaller n_e is given by a gas with the larger t_i because, in Eq. (8), term 2 is dominant for the major part of the pulse duration in the pressure region of interest, as described already. Therefore, if we ignore the variation of $Q_m\bar{\epsilon}^{1/2}$ among gases,

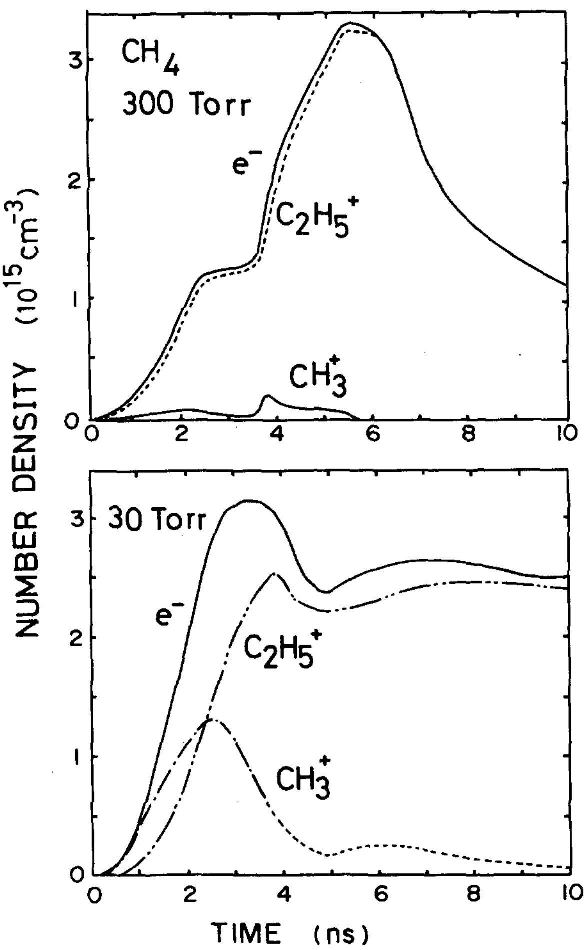

FIG. 11. The calculated number densities of secondary electrons e^-, monomer ion CH_3^+, and dimer ion $C_2H_5^+$ as functions of time for 30 and 300 Torr of CH_4.

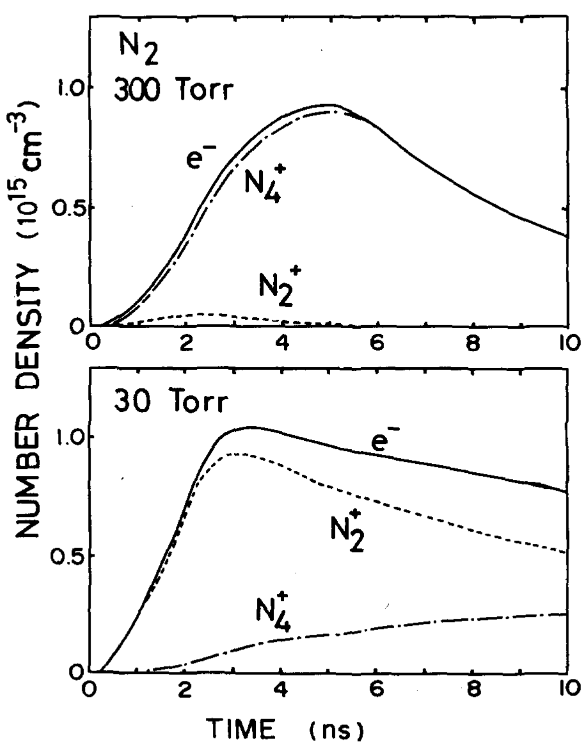

FIG. 10. The calculated number densities of secondary electrons e^-, monomer ion N_2^+, and dimer ion N_4^+ as functions of time for 30 and 300 Torr of N_2.

the larger D_{obs} is given by a gas with the larger t_i or pt_i at the same pressure under the larger E_z/p, as described above. This is the principal conclusion on the relationship between D_{obs} and t_i. Hereafter, data on D_{obs} for various polyatomic gases will be analyzed on the basis of this conclusion. The value of D_{obs} can give information on t_i for the pulse duration, which is difficult to be measured directly.

The E/p–pt_i curves for several gases have been obtained experimentally by Felsenthal and Proud[4] as seen in Fig. 16 of Ref. 4 in which pt_i increases with decreasing E/p. The above conclusion suggests that the E/p–pt_i curve for a gas giving the larger D_{obs} at the same pressure must be placed at the upper side in such a figure. In fact, in Fig. 16 of Ref. 4, the values of E/p at the same pt_i are in the order

$$CCl_2F_2 > SF_6 > N_2 > O_2 > Ar > He \; . \tag{11}$$

This is the same order as for D_{obs} at the same pressure as seen in Figs. 6 and 7 of Ref. 5. The relationship between He and Ar has been discussed in part I.[1]

As demonstrated by Felsenthal and Proud,[4] the value of t_i for a gas with no experimental value of t_i can be determined by Eq. (6) from swarm parameters (w, α/p, and η/p). Values of η/p have been measured as functions of E/p for some gases. According to references, values of η/p are in the order[31–34]

$$SF_6 \approx CCl_2F_2 \gg N_2O > O_2 \gg CO_2 \tag{12}$$

and ratios of η/α are in the order

$$CCl_2F_2 \gtrapprox SF_6 > N_2O > O_2 > CO_2 \; . \tag{13}$$

For $E/p > 60$ V cm^{-1} Torr^{-1}, the ratio of η/α is negligibly small for O_2 and CO_2. On the other hand, since the number density of gas molecules is 3.3×10^{18} cm^{-3} at 20 °C and 100 Torr, the half-life of secondary electrons for electron-attachment processes is less than 1 ns for the rate constant larger than 2×10^{-10} cm^3/s. Such large rate constants are reported for O_2 (3.4×10^{-10} cm^3/s at 6.7 eV[35]), N_2O (9.2×10^{-10} cm^3/s at 2.4 eV[35]), SF_6 (2×10^{-7} cm^3/s at thermal energy[36]), and CCl_2F_2 (5.6×10^{-9} cm^3/s at 1.08 eV[36]). Then, the contribution of electron-attachment processes may be important in CCl_2F_2, SF_6, and N_2O. In fact, as seen in Fig. 7 of Ref. 5, values of D_{obs} in these gases are larger than in other gases; they are in the order

$$CCl_2F_2 > SF_6 > N_2O > CH_4 \; , \tag{14}$$

as predicted from the ordering (12) and (13). This fact suggests that t_i is lengthened due to the large η/p in Eq. (6).

For the gas with no appreciable electron-attachment process, the value of pt_i can be estimated as $p/w\alpha$. Although E/p varies with t and p, from Figs. 6–8, we attempt to estimate the value of $p/w\alpha$ at 100 V cm^{-1} $\times$ Torr^{-1} as the representative value for gas pressures between 20 and 50 Torr. From data on w and α/p in Ref. 8, values of $p/w\alpha$ are in the order

$$N_2 > CO_2 > CH_4 > O_2 > H_2 \; . \tag{15}$$

This order is almost the same with the order of D_{obs} in Fig. 7 of Ref. 5 except CH_4 because D_{obs} for CH_4 is rather larger than for N_2. This fact supports the present conclusion on the relationship between D_{obs} and t_i. D_{obs} for CH_4 is attributed to the large value of $Q_m \bar{\epsilon}^{1/2}$ for CH_4 as described already.

On the other hand, for the gas with no electron-attachment process, the value of pt_i can also be estimated by the following equation instead of $p/w\alpha$:

$$\frac{1}{n_0 t_i} = \left(\frac{2}{m}\right)^{1/2} \int_{\mathrm{I.P.}}^{\infty} \epsilon^{1/2} \sigma_i(\epsilon) F(\epsilon) d\epsilon \; , \tag{16}$$

where I.P. is the ionization potential of a gas, $\sigma_i(\epsilon)$ the total ionization cross section of a gas for electrons with energy ϵ, and $F(\epsilon)$ the distribution function of ϵ. Data on σ_i for lower-energy electrons are given by Rapp and Englander-Golden.[26] Equation (16) indicates that, at the same pressure, the larger D_{obs} or t_i is given by the gas with the higher I.P., the slower initial slope of σ_i, and the larger distribution of ϵ at the lower energy.

There are few available data on $F(\epsilon)$ in the E/p region of interest. We can find some data on D_L/μ as functions of E/p between 50 and 100 V cm^{-1} Torr^{-1} for estimation of $\bar{\epsilon}$ for H_2,[10] N_2,[13] O_2,[37] CO_2,[38] CH_4,[18] SF_6,[39] and CCl_2F_2.[40] Values of $\bar{\epsilon}$ for these gases estimated on the assumption of the Maxwellian are about 7–8 eV except CCl_2F_2 (5.5 eV) at 100 V cm^{-1} Torr^{-1} and are in the order

$$CH_4 > H_2 \approx O_2 \approx CO_2 \approx (SF_6) > N_2 > (CCl_2F_2) \tag{17}$$

at 50 V cm^{-1} Torr^{-1}. The values for SF_6 and CCl_2F_2 are extrapolated from data at E/p above 100 V cm^{-1} Torr^{-1}.

Let us suppose that ϵ is lowered by $Q_t f$, where Q_t is the total collision cross section and f the mean fractional energy loss per collision which is given by[41]

$$f = 1.74\times 10^{-14} w^2 / k_T \; , \tag{18}$$

where k_T is the Townsend energy factor ($k_T = 39.8\, D_L/\mu$ at 20 °C[11] for the Maxwellian). Values of $Q_t f$ from Eq. (18) are shown as functions of $\bar{\epsilon}$ in Fig. 12. Data on Q_t are cited from references as follows; H_2,[42] N_2,[20] O_2,[43,44] CO_2,[20] CH_4,[19] and SF_6.[45] When the curves in Fig. 12 are compared with the ordering (17), the high value of $\bar{\epsilon}$ for CH_4 at lower E/p is attributed to the small value of $Q_t f$ at lower $\bar{\epsilon}$ because of the special dependence of D_L/μ on E/p[18]; the low value of $\bar{\epsilon}$ for N_2 is attributed to the large value of $Q_t f$, and the intermediate values for O_2, CO_2, and SF_6 are also understood by their curves of $Q_t f$ from Eq. (18). This means that $Q_t f$ from Eq. (18) is useful to estimate $F(\epsilon)$ qualitatively, though there is some problem for the application of Eq. (18) to the higher E/p region.

Now, we examine the order of D_{obs} as seen in Fig. 7 of Ref. 5 on the basis of Eq. (16). When data on I.P. and σ_i are compared for N_2O and N_2, t_i for N_2O must be smaller than for N_2 because of the large $Q_t f$ for N_2. However, D_{obs} for N_2O is larger than for N_2. This fact suggests that D_{obs} or t_i for N_2O may be affected appreciably by the electron-attachment process which is ignored in Eq. (16). Similarly, in the comparison between CH_4 and N_2, D_{obs} for CH_4 rather larger than for N_2 can be explained only by the large $Q_m(\bar{\epsilon})\bar{\epsilon}^{1/2}$ for CH_4. The value

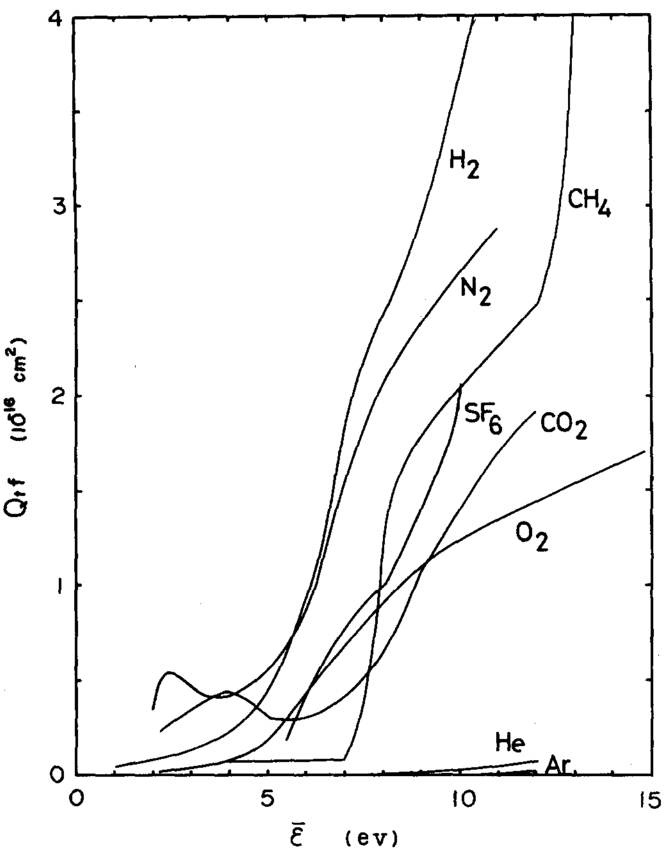

FIG. 12. The estimated values of $Q_t f$ (Q_t: total collision cross section for electrons; and f: mean fractional energy loss per collision) as functions of the mean electron energy.

of D_{obs} for N_2 rather larger than for CO_2 is attributed to the higher I. P., the smaller σ_i, and the larger $Q_t f$ for N_2 than for CO_2. The value of D_{obs} for O_2 smaller than for CO_2 is attributed to the lowest I. P. among gases compared in the ordering (15). On the other hand, for H_2, the value of D_{obs} is the lowest among polyatomic gases as seen in Fig. 7 of Ref. 5. This fact can be interpreted in terms of $p/w\alpha$ as seen in the ordering (15) because of the largest α/p for H_2 at 100 $V\,cm^{-1}\,Torr^{-1}$. However, the largest α/p cannot be derived from Eq. (16) because H_2 has a high I. P., a small σ_i, and a large $Q_t f$.

ACKNOWLEDGMENTS

The authors wish to express their thanks to Sin-ichi Sato and Minoru Maeda of Fujitsu Ltd. at the Computing Center of Tokai Research Establishment, JAERI for their valuable advice and help in programming and computation.

[1]H. Arai and H. Hotta, J. Chem. Phys. 75, 2252 (1981).
[2]R. Tanaka, H. Sunaga, and H. Hotta, Radiat. Res. 63, 14 (1975).
[3]F. F. Rieke and W. Prepejchal, Phys. Rev. A 6, 1507 (1972).
[4]P. Felsenthal and J. M. Proud, Phys. Rev. Sect. A 139, 1796 (1965).
[5]H. Hotta and H. Arai, J. Chem. Phys. 67, 3608 (1977).
[6]H. Hotta, R. Tanaka, and H. Arai, Radiat. Res. 63, 32 (1975).
[7]H. Arai and H. Hotta, Radiat. Res. 64, 407 (1975).
[8]J. Dutton, J. Phys. Chem. Ref. Data 4, 577 (1975).
[9]D. J. Rose, Phys. Rev. 104, 273 (1956).
[10]N. Kontoleon, J. Lucas, and L. E. Virr, J. Phys. D 5, 956 (1972).
[11]A. L. Gilardini, *Low Energy Electron Collisions in Gases* (Wiley-Interscience, New York, 1971).
[12]S. C. Haydon and O. M. Williams, J. Phys. D 9, 523 (1976).
[13]N. Kontoleon, J. Lucas, and L. E. Virr, J. Phys. D 6, 1237 (1973).
[14]X. Fink and P. Huber, Helv. Phys. Acta 38, 717 (1965).
[15]H. Schumbohm, Z. Phys. 182, 317 (1965).
[16]L. Frommhold, Z. Phys. 156, 144 (1959).
[17]A. E. D. Heylen, J. Chem. Phys. 38, 765 (1963).
[18]C. S. Lakshiminarasimha and J. Lucas, J. Phys. D 10, 313 (1977).
[19]Y. Itikawa, At. Data Nucl. Data Tables 14, 1 (1974).
[20]H. H. Landolt and R. Börnstein, *Zahlenwerte und Funktionen* (Springer, Berlin, 1956), Vol. 1, Part 1.
[21]D. Auerbach, R. Cacak, R. Caudano, T. D. Gaily, C. J. Keyer, J. Wm. McGowan, J. B. A. Mitchell, and S. F. J. Wilk, J. Phys. B 10, 3797 (1977).
[22]P. Mul and J. Wm. McGowan, J. Phys. B 12, 1591 (1979).
[23]P. Mul and J. Wm. McGowan, in "Compilation of Data Relevant to Rare Gas–Rare Gas and Rare Gas–Monohalide Excimer Lasers," Technical Report H-78-1, Vol. 1, edited by E. W. McDaniel, M. R. Flannery, H. W. Ellis, F. L. Eisele, W. Pope, and T. G. Roberts, U. S. Army Missile Research and Development Command, Redstone Arsenal, Alabama (1979).
[24]A. Good, Chem. Rev. 75, 561 (1975).
[25]R. P. Clow and J. H. Futrell, Int. J. Mass Spectrom. Ion Phys. 4, 165 (1970).
[26]D. Rapp and P. Englander-Golden, J. Chem. Phys. 43, 1464 (1965).
[27]P. Englander-Golden and D. Rapp, Lockheed Missiles and Space Company Report No. LMSC 6-74-64-12, Palo Alto, California (1964).
[28]J. N. Bardsley and M. A. Biondi, Adv. At. Mol. Phys. 6, 1 (1970).
[29]D. E. Wilson and D. A. Armstrong, Can. J. Chem. 48, 598 (1970).
[30]H. N. Maier and R. W. Fessenden, J. Chem. Phys. 62, 4790 (1975).
[31]M. S. Bhalla and J. D. Craggs, Proc. Phys. Soc. London 80, 151 (1962) (SF_6).
[32]M. A. Harrison and R. Geballe, Phys. Rev. 91, 1 (1953) (CCl_2F_2 and O_2).
[33]J. Dutton, F. M. Harris, and D. B. Hughes, J. Phys. B 8, 313 (1975) (N_2O).
[34]V. J. Conti and W. Williams, J. Phys. D 8, 2198 (1975) (CO_2).
[35]L. G. Christophorou, *Atomic and Molecular Radiation Physics* (Wiley-Interscience, New York, 1971).
[36]L. G. Christophorou, Chem. Rev. 76, 409 (1976).
[37]J. Lucas, D. A. Price, and J. M. Moruzzi, J. Phys. D 6, 1503 (1973).
[38]C. S. Lakshiminarasimha, J. Lucas, and N. Kontoleon, J. Phys. D 7, 2545 (1974).
[39]M. S. Naidu and A. N. Prasad, J. Phys. D 5, 1090 (1972).
[40]M. S. Naidu and A. N. Prasad, J. Phys. D 2, 1431 (1969).
[41]L. G. Christophorou, K. S. Gant, and J. K. Baird, Chem. Phys. Lett. 30, 104 (1975).
[42]D. E. Golden, Phys. Rev. 146, 40 (1966).
[43]A. Salop and H. H. Nakano, Phys. Rev. A 2, 127 (1970).
[44]S. Trajmar, D. C. Cartwright, and W. W. Williams, Phys. Rev. A 4, 1482 (1971).
[45]R. E. Kennerly, R. A. Bonham, and M. McMillan, J. Chem. Phys. 70, 2039 (1979).